Doctor of Philosophy

Cortical interneuron paucity and altered PTEN/PI3K/AKT pathway in an infant rat model of malformation of cortical development

영아기 대뇌피질발달기형 동물모델에서 억제성 신경세포의 결핍과 PTEN/PI3K/AKT경로의 이상

The Graduate School

of the University of Ulsan

Department of Medicine

Minyoung Lee

Cortical interneuron paucity and altered PTEN/PI3K/AKT pathway in an infant rat model of malformation of cortical development

Supervisor: Mi-Sun Yum

A Dissertation

Submitted to
The Graduate School of the University of Ulsan
In partial Fulfillment of the Requirements
for the Degree of

Doctor of Philosophy

By

Minyoung Lee

Department of Medicine
Ulsan, Korea
August 2019

Cortical interneuron paucity and altered PTEN/PI3K/AKT pathway in an infant rat model of malformation of cortical development

This certifies that the Doctor of Philosophy of

Minyoung Lee is approved.

Tae-Sung Ko (signature)
Committee Chair Dr.

Mi-Sun Yum (signature)
Committee Member Dr.

Peter C.W. Lee (signature)
Committee Member Dr.

Dong-Cheol Woo (signature)
Committee Member Dr.

Eun-Hee Kim (signature)
Committee Member Dr.

Department of Medicine

Ulsan, Korea

August 2019

Abstract

Cortical interneuron paucity and altered PTEN/PI3K/AKT pathway in an infant rat model of malformation of cortical development

Minyoung Lee

Department of Medicine, the Graduate School of University of Ulsan

Background: Malformations of cortical development (MCDs) is one of the major causes of intractable epilepsies such as epileptic spasms. Rats with prenatal exposure to methylazoxymethanol (MAM) have been used as a model of malformation of cortical development (MCD) and increased seizure susceptibility to N-methyl-D-aspartate (NMDA) during infancy was also shown in this model.

Objective: The aim of this study is to identify the pathologic changes and in vivo neurometabolic alterations in rat model MCD during infancy. Underlying molecular changes were also explored to understand the mechanisms of the enhanced seizure susceptibility during infancy in MCD rat model.

Methods: At gestational day 15, two dosages of MAM (15mg/kg IP) were injected to pregnant rats to produce MCD and normal saline to controls. The offspring underwent in vivo magnetic resonance imaging including ^{1}H-MR spectroscopy (^{1}H-MRS), diffusion tensor imaging (DTI), and chemical exchange saturation transfer of glutamate (GluCEST) at postnatal day (P) 15 using a 7T small-animal imaging system. On the same day, those animals were sacrificed and protein expression of the PI3K/AKT/mTOR pathway was measured from the cortex. Another set of prenatally MAM-exposed rats were pretreated with two different dosing regimens of rapamycin (3 or 10mg/kg, P5 to P14 or P9 to P14) and the number and onset of spasms were monitored for 90 minutes after the NMDA (15mg/kg i.p.) injection at P15.

Results: At P15, immunofluorescence staining of retrosplenial cortices of rats with MCD revealed decreased cells with neuronal nuclei (NeuN), parvalbumin, and reelin expression. ^{1}H-MRS and GluCEST imaging of retrosplenial cortex showed reduction of glutamate (Glu, p = 0.002), glutamate-plus-glutamine (Glu+Gln, p = 0.017), N-

acetylaspartate (NAA, p = 0.002), N-acetylaspartate-plus-N-acetylaspartylglutamate (NAA+NAAG, p = 0.004), and macromolecules (MM) and lipids (Lips, $p < 0.05$) and the level of GluCEST (%, $p < 0.001$) in rats with MCD. There was translational deactivation of phosphatase and tensin homolog (PTEN), Akt, FoxO3a, and GSK3β in rats with MCD. Rapamycin pretreatment did not affect the NMDA-triggered spasm susceptibility and there was no significant change of pS6/S6, S6, Rictor, and PI3k expression in cortices of rats with prenatal MAM exposure.

Conclusion: In prenatally MAM exposed infant rats, abnormal cortical migration with decreased GABAergic interneurons and comparable in vivo MR imaging characteristics were identified. Prenatal MAM exposure also leads to alteration of PTEN/PI3K/AKT pathway during their infancy, which can be further investigated as the target of MCD-related epilepsy treatment.

KEY WORDS: methylazoxymethanol acetate (MAM), malformation of cortical development (MCD), PTEN, AKT, animal model

Contents

List of Tables and Figures

List of Abbreviations

AKT = Protein kinase B

CV = Cresyl violet staining

DTI = Diffusion tensor imaging

FA = Fractional anisotropy

FCD = Focal cortical dysplasia

FoxO3a = Forkhead box protein O3a

GABA = Gamma-aminobutyric acid

GAD65 = Glutamate decarboxylase 65

Gln = Glutamine

GluCEST = Chemical exchange saturation transfer of glutamate

Glu = Glutamate

GSK3β = Glycogen synthase kinase 3 beta

G15 = Gestational day 15

HMEG = Hemimegalencephaly

IF = Immunofluorescence staining

IP = Intraperitoneal injection

Lips = Lipids

MAM = Methylazoxymethanol

MAP2 = Microtubule-associated protein 2

MBP = Myelin basic protein

MCD = Malformation of cortical dysplasia

MEG = Megalencephaly

MMs = Macromolecules

MRS = Magnetic resonance spectroscopy

mTOR = Mammalian target of rapamycin

NAA = N-acetylaspartate

NAAG = N-acetylaspartylglutamate

NeuN = Neuronal nuclei

NMDA = N-methyl-D-aspartic acid

PI3K = Phosphatidylinositol-4, 5-bisphosphate 3-kinase

PTEN = Phosphatase and tensin homolog

PV = Parvalbumin

P15 = Postnatal day 15

p-Akt = phosphorylated Akt

p-PTEN = phosphorylated PTEN

p-S6 = phosphorylated S6 ribosomal protein

RSC = Retrosplenial cortex

S6 = S6 ribosomal protein

TSC = Tuberous sclerosis complex

^{1}H-MRI = Proton nuclear magnetic resonance imaging

Introduction

The cerebral cortex, the largest area of the cerebrum, plays an important role in memory, language, cognition, and thinking[1)]. With its vast synaptic connections of many cells, cerebral cortex is well organized with six layers of spiny excitatory neurons and GABAergic interneurons[1-4)]. The developmental process of the cerebral cortex is accomplished through well-orchestrated neurogenesis, cell proliferation, neuronal migration, and organization involving various transcription factors and proteins[1, 3)] and their disruption result in a broad spectrum disease, malformations of cortical development (MCDs). Many genetic or environmental insults[2, 5)] can cause the MCDs and patients with MCD suffer from developmental problems, neurological deficits, and epilepsy[3, 6-8)]. Especially, MCD is the most common cause of intractable epilepsy in pediatric populations [6, 9, 10)]. To conquer these intractable epilepsies associated with MCD, the epileptogenic mechanisms in MCD should be identified. As epileptogenesis of these malformed brain is still unclear[11, 12)], many clinical and translational researches are underway and researches using various animal models

are one of them[3),11, 12)]. Methylazoxymethanol (MAM), a cytotoxic agent involved in DNA methylation and alkylation[6, 11, 13, 14)], has an antimitotic effect that specifically eliminated neuronal precursors undergoing mitosis and indirectly affects glial cells, resulting in abnormalities of cell proliferation and migration[11, 13)]. The offspring from MAM-treated rats have developmental brain anomalies including migration failure, ventricular enlargement, and disorganization of neocortical and hippocampal structures[11, 13, 15)], which resemble the pathologic findings observed in patients with MCD[6, 15)]. Thus, MAM induced MCD model[5, 14)] was chosen for this study. Previous study of our group also reported cognitive impairment and increased seizure susceptibility during infancy in this MAM-induced MCD rat model[6)].

On the other hand, molecular studies with patients with MCD and animal models revealed mutations in PI3K/AKT/mTOR pathway as one of the genetic basis linked to brain malformations[16-21)]. PI3K/AKT/mTOR pathway and its negative regulator, PTEN, play an important role in the neurodevelopment of cerebral neocortex such as radial migration, plasticity and soma size[19, 22)] and the disruption

of this pathway is known to be associated with MCD and other related disorders[23-25].

Using a model of MAM-induced MCD rats, this study aimed to identify pathological changes and in vivo MR features during infancy. It was also hypothesized that prenatal exposure to MAM results in malformed brain with molecular changes of PI3K/AKT/mTOR pathway, which may be associated with seizure susceptibility of this model. Translational changes of PI3K/AKT/mTOR pathway were explored and pretreatment of rapamycin on spasms susceptibility was tested in infant rats with MCD.

Methods

Animals

Experiments were approved by the Institutional Animal Care and Use Committee of the Ulsan University College of Medicine and conformed to the Revised Guide for the Care and Use of Laboratory Animals [8th Edition, 2011]. Timed-pregnant Sprague-Dawley rats were purchased (Orient Bio Inc., Seoul, Korea) at gestational day 14 (G14) and housed individually in the animal facility. Rats were housed with 12h light/dark cycle and free access to food and water under aseptic condition. On G15, two dosages of MAM (15mg/kg intraperitoneally, MRIglobal, Missouri) were injected to pregnant rats and normal saline to controls at 08:30 and 18:30. Delivery occurred consistently on gestational day 21, which was considered postnatal day (P) 0 for the offspring.

The overall experimental schedule was described in Figure 1.

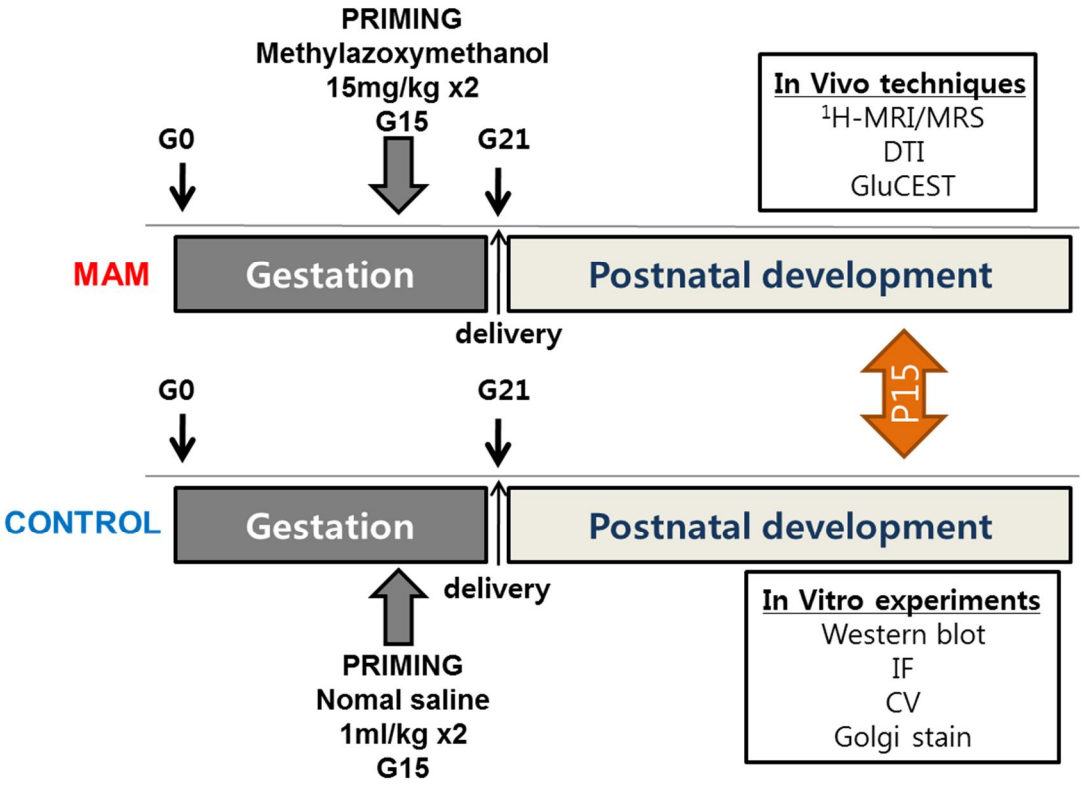

Figure 1. The timeline of experimental procedures.

In vivo techniques

	^{1}H-MRI/MRS		DTI		GluCEST		Cortical length	
	Control	MAM	Control	MAM	Control	MAM	Control	MAM
Male	9	5	15	9	3	4	18	13
Female	1	5	1	6	5	4	6	10
Total	10	10	16	15	8	8	24	23

In vitro experiments

	Western blot		IF		Cresyl violet		Golgi stain	
	Control	MAM	Control	MAM	Control	MAM	Control	MAM
Male	18	11	7	6	6	7	2	2
Female	14	13	8	5	5	8	3	3
Total	32	24	15	11	11	15	5	5

Rapamycin pretreatments

	10 days (P5-P14)		6 days (P9-P14)	
	VEH	3mg/kg Rap.	VEH	10mg/kg Rap.
Male	4	1	4	7
Female	0	2	4	3
Total	4	3	8	10

Table 1. Summary of the number of rats used in experiments.

Rapamycin pretreatment and NMDA-induced spasms

To evaluate the response to pretreatment of rapamycin on NMDA-induced spasms, prenatally MAM-exposed rats were pretreated with 10mg/kg rapamycin (LC Lab., USA) at P9 for 6 days (n = 10), 3mg/kg rapamycin at P5 for 10 days (n = 3) or

vehicle (2% ethyl alcohol; 6 days, n = 8; 10 days, n = 4). In those animals with pretreatments, spasms were triggered by intraperitoneal injection of NMDA (15mg/kg) at P15 and the number of spasms, the latencies to onset of spasms were monitored.

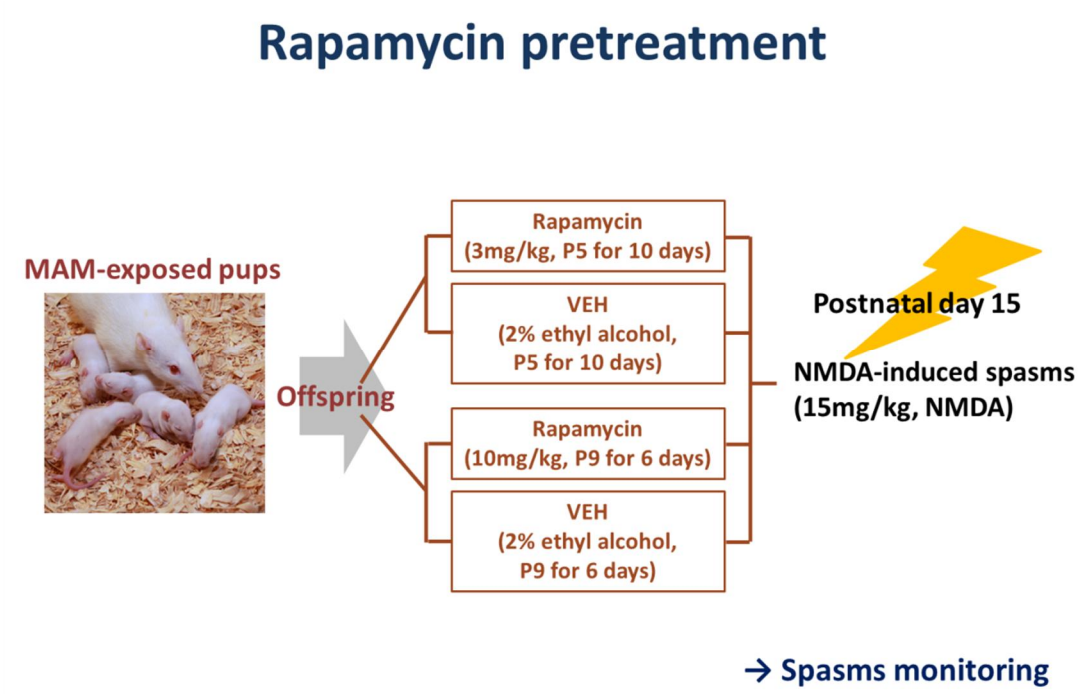

Figure 2. Rapamycin pretreatment against NMDA triggered spasms

In Vivo Magnetic Resonance Imaging Studies

Animals were maintained under anesthesia with 1% isoflurane in a 1:2 mixture of O_2:N_2O with monitoring of their respiratory rate, electrocardiogram, and rectal temperature. MR images were obtained using a 7.0 T/160-mm bore animal MRI system (Bruker Pharmascan, Ettlingen, Germany) with Paravision 6.0.1.software in a configuration of a 72-mm transmit volume coil and a mouse brain surface receiver coil, respectively. Axial T2 weighted images were covered from the cervical spinal cord to the olfactory bulb.

Diffusion tensor images (DTI) were acquired using a four-shot DT-echo planar imaging sequence (TR = 3.7s, TE = 20ms, B0 = 1000 s/mm^2) with a 10-ms interval (Δ) between the application of diffusion gradient pulses, a 4-ms diffusion gradient duration (δ), a gradient amplitude (G) of 46.52 mT/m, and the Jones 30 gradient scheme. Postprocessing analysis was performed using Diffusion Toolkit software (http://trackvis.org/). The retrosplenial cortex of each rat was selected and the fractional anisotropy (FA) and mean diffusivity (MD) were calculated from the

diffusion tensor parametric maps.

GluCEST images were acquired from an axial slice (1㎜ thick) that at 3mm posterior to bregma. GluCEST images were acquired using T_2-weighted imaging (rapid acquisition with relaxation enhancement [RARE]) with a frequency selective saturation preparation pulse comprised a Gaussian pulse and a total duration of 1000 ms (irradiation offset of 500.0 Hz and interpulse delay of 10 μs) at a B_1 peak of 5.6 μT. Z-spectra were obtained from –5.0 ppm to +5.0 ppm with intervals of 0.33 ppm (total, 31 images). The sequence parameters were as follows: repetition time/echo time (TR/TE) = 4200/36.4 ms, field of view = 30 × 30 mm^2, slice thickness = 1 mm, matrix size = 96 × 96, RARE factor = 16, echo spacing = 6.066 ms, and average = 1. To measure the GluCEST (%), the regions of interest, manually drawn on the retrosplenial cortex in T_2-weighted anatomical MR images, were overlaid on the GluCEST maps. GluCEST contrast is measured as the asymmetry between an image obtained with saturation at the resonant frequency of exchangeable amine protons (+3 ppm downfield from water for glutamate) and an image with saturation

equidistant upfield from water (–3 ppm), according to the following equation:

$$\mathbf{GluCEST}\ (\%) = \frac{\boldsymbol{S}_{-3.0\ ppm} - \boldsymbol{S}_{+3.0\ ppm}}{\boldsymbol{S}_{-3.0\ ppm}} * \mathbf{100}$$

where $\boldsymbol{S}_{\text{-3.0ppm}}$ and $\boldsymbol{S}_{\text{+3.0ppm}}$ are the magnetizations obtained with saturation at a specified offset from the water resonance of 4.7 ppm. The B0/B1 maps on the same slices were acquired for B_0 and B_1 correction. The B_0 map was calculated by linearly fitting the accumulated phase per pixel following phase unwrapping against the echo time differences from gradient echo (GRE) images collected at TEs of = 1.9 and 2.6 ms. B_1 maps were calculated by using the double-angle method (flip angles 30° and 60°) and the linear correction for B_1 was calculated as the ratio of the actual B_1 to the expected value.

^{1}H-MRS was performed at P15 in MAM-exposed rat (n = 10) and control (n = 10). The MR spectra were acquired through a signal voxel (from bregma to –3.0 mm in a coronal section, 1.2 × 1.3 × 3 mm^3; Fig. 3A) in the retrosplenial cortex using a point-resolved spectroscopy (PRESS) sequence for 128 acquisitions with TR/TE = 5000/13.4 ms. For quantification, unsuppressed water signals were also acquired

from the same voxel (average = 8). All the MR spectra were processed with the linear combination analysis method (LC Model ver. 6.0, Los Angeles, CA) to calculate the metabolite concentrations from a fit to the experimental spectrum, based on a simulated basis set. The following brain metabolites were included in the metabolite basis set: alanine (Ala), aspartate (Asp), creatine (Cr), ɣ-aminobutyric acid (GABA), glucose, glutamate, glutamine, glycerophosphorylcholine, phosphorylcholine, myo-inositol (mIns), lactate (Lac), phosphocreatine (PCr), N-acetylaspartate (NAA), N-acetylaspartylglutamate (NAAG), taurine, macromolecules (MMs), and lipids. The water-suppressed time domain data were analyzed between 0.2 and 4.0 ppm, without further T1 or T2 correction. Absolute metabolite concentrations (mmol/kg wet weight) were calculated using the unsuppressed water signal as an internal reference (assuming 80% brain water content) [26]. The in vivo proton spectra were judged to have an acceptable value if the standard deviation of the fit for the metabolite was less than 20%.

Measurement of cortical neurons and morphology analysis

The MAM-exposed rats and the corresponding controls were transcardially perfused with 4% paraformaldehyde on P15 under deep anesthesia, and their brains were removed and cryoprotected with phosphate-buffered saline (PBS) containing from 10% to 30% sucrose until sink. Twenty-micron serial coronal sections were cut on a cryocut microtome then sections were mounted on silane coated slides and stored at -80℃ for staining procedures.

For cresyl violet staining, the sections were fixed for 15min for 4% paraformaldehyde solution and defatted in 70% ethanol solution containing 0.5% acetic acid for 5min and washed. Then, these were dipped in 0.3% cresyl violet solution for 3min and washed. The slides were mounted in cover glasses and analyzed by light microscopy (Olympus BX-53) with a digital camera (Olympus microscope digital camera, 5M CCD).

The modified Golgi-Cox impregnation was performed according to instructions of the manufacturer using FD Rapid GolgiStain kit (FD NeuroTechnologies, Ellicott

City, MD). Postnatal day 15-old rat brains were rinsed with distilled water for remove blood and trimmed to approximately 1 cm thickness. The tissue was immersed in impregnation solution for 2 weeks, transferred to solution C for 3 to 4 days, and a cryostat was used for cutting at 120㎛. The sections were mounted on silane coated slides (5116-20F, MUTO PURE CHEMICAL) and stained with solution D and E. Then slides were moved for dehydration and mounted with Permount mounting medium (ThermoFisher scientific, USA). The Golgi-impregnated cortical neurons were analyzed at 100x and 200x magnification using Olympus CellSens standard 1.13 and Image J software. The number of cortical neurons was measured at 100x magnification with focus on retrosplenial cortex and two pyramidal neurons were selected to evaluate the length of apical dendrites and the number of the second branches of basal dendrites at 200x magnification. The Pyramidal neurons were selected according to the following criteria: 1) triangular shaped soma; 2) one apical dendrite; and 3) basal dendrites, and non-pyramidal neurons were counted as interneurons.

Immunofluorescence and western blot analysis

After heating on hot plate at 50℃ for 20min for antigen-retrieval, the slides were washed and incubated in blocking solution (containing 5% normal host serum and 0.1% BSA/0.3% Triton X-100) for 1 hour. Primary antibody (anti-MBP and anti-parvalbumin; abcam, anti-MAP2, anti-NeuN, and anti-Reelin; EMD Millipore) with blocking solution at 4℃ for 24h fluorescein secondary antibody (Fluorescein anti-mouse IgG, fluorescein anti-rabbit IgG and Cy®3 anti-rabbit IgG; Vector lab, Alexa fluor 594 anti-rat IgG; Thermo fisher) were serially applied for 1hour at room temperature. After washing three times, slides were mounted in cover glasses and analyzed by fluorescence microscopy (Olympus BX-53). Images were acquired with a digital camera (Olympus microscopy digital camera, 5M CCD).

For western blot analysis, bilateral cortical tissues from bregma to posterior hippocampal area without hippocampus (anterior posterior 0 to -5 mm) were obtained from control and MAM-exposed rats at P15. Isolated tissues from each rat were homogenized with Pro-prep (intron biotechnology, 17081) at −4°C ice bath and

the protein samples were quantified with BSA. The acquired proteins were separated with sodium dodecyl sulfate polyacrylamide gel electrophoresis and transferred to PVDF membrane. The membranes were blocked in 10% skim milk in tris-buffered saline with Tween-20 (TBST solution) for 1h at room temperature. After then, the membranes incubated for overnight at 4 ºC with following primary antibodies; anti-NeuN (EMD Millopore), anti-GAD65 (EMD Millopore), anti-parvalbumin (abcam), anti-PI3k (Cell signaling, Technology, Inc.), anti-Rictor (Cell signaling, Technology, Inc.), anti-S6 (Cell signaling, Technology, Inc.), anti-p-S6 (Cell signaling, Technology, Inc.), anti-p-PTEN (Cell signaling, Technology, Inc.), anti-PTEN (Cell signaling, Technology, Inc.), anti-p-Akt (Cell signaling, Technology, Inc.), anti-Akt (Cell signaling, Technology, Inc.), anti-FoxO3a (Cell signaling, Technology, Inc.), anti-GSK3β (Cell signaling, Technology, Inc.), and anti-β-actin (Santa Cruz Biotechnology, Inc.) was used as a loading control. Then, the membranes were incubated 90 min in anti-rabbit IgG, horseradish peroxidase (HRP)-linked antibody (Cell signaling, Technology, Inc.) or anti-mouse IgG, HRP antibody (Enzo) at room

temperature. Membranes were further rinsed with TBST and followed by development using ECL solution (Bio-rad, clarity western ECL substrate) on fusion solo S (Vilber Lourmat SAS, France). Normalization was performed by developing parallel western blots probed with beta-actin antibody and analyzed by densitometry using Evolution-Capt (Fusion software, Vilber Lourmat SAS, France).

Western blot

Antibody name	Host[#]	Clonality*	Catalog No.	Company
Akt (pan)	M	M	2920	Cell signaling
FoxO3a	Rb	M	12829	Cell signaling
GAD65	Rb	Unknown	ABN101	Millipore
GSK3bata	M	M	9832	Cell signaling
NenN	M	M	MAB377	Millipore
PI3 Kinase p110α	Rb	M	4249	Cell signaling
Parvalbumin	Rb	P	ab11427	Abcam
PTEN	M	M	9556	Cell signaling
Rictor	Rb	M	2114	Cell signaling
S6 Ribosomal Protein	M	M	2317	Cell signaling
Phospho-Akt (Ser473)	Rb	M	4060	Cell signaling
Phospho-PTEN (Ser380)	Rb	P	9551	cell signaling
Phospho-S6 Ribosomal Protein	Rb	M	4858	Cell signaling
β-Actin	M	M	sc-47778	Santa Cruz

[#]Host: M, mouse; Rb, rabbit

*Clonality: M, monoclonal antibody; P, polyclonal antibody

Immunofluorescence

Antibody name	Host[#]	Clonality*	Catalog No.	Company
Myelin Basic Protein Ab	Rat	M	ab7349	Abcam
MAP-2	Rb	P	AB5622-1	Millipore
NenN	M	M	MAB377	Millipore
Parvalbumin	Rb	P	ab11427	Abcam
Reelin	M	M	MAB5364	Millipore

[#]Host: M, mouse; Rb, rabbit

*Clonality: M, monoclonal antibody; P, polyclonal antibody

Table 2. The list of antibodies used.

Statistical analysis

Using IBM SPSS (ver. 22.0; IBM Corp., Armonk, NY, USA), statistical analyses were performed. Level of significance was preset to $p < 0.05$. Two group comparisons of the concentrations of metabolites, cortical neuron analysis and rapamycin treatment data used the Mann-Whitney's *U* test. Student's *t*-test was used for protein expression data following normal distribution in two-group comparisons. Repeated measures ANOVA and *t*-tests were conducted to test for the treatment effect of the different diffusion parameters.

Results

Cortical interneurons & dendritic arborization of pyramidal cells of RSC in this infant rat model of MCD

At P15, the structural changes caused by prenatal MAM exposure are confirmed by cresyl violet staining (Fig 3A). Immunofluorescence staining of retrosplenial cortex (RSC) of rats with MCD shows decreased expression of MBP and MAP2 (Fig. 3B) and reduced numbers of neurons including GABAergic interneurons when compared to controls (Fig. 3C). Western blots also showed significantly decreased protein expressions of neuronal or GABAergic inhibitory neuronal markers in rats with MCD (Fig. 3D, NeuN; $p < 0.001$, GAD65; $p = 0.003$, parvalbumin; $p < 0.001$).

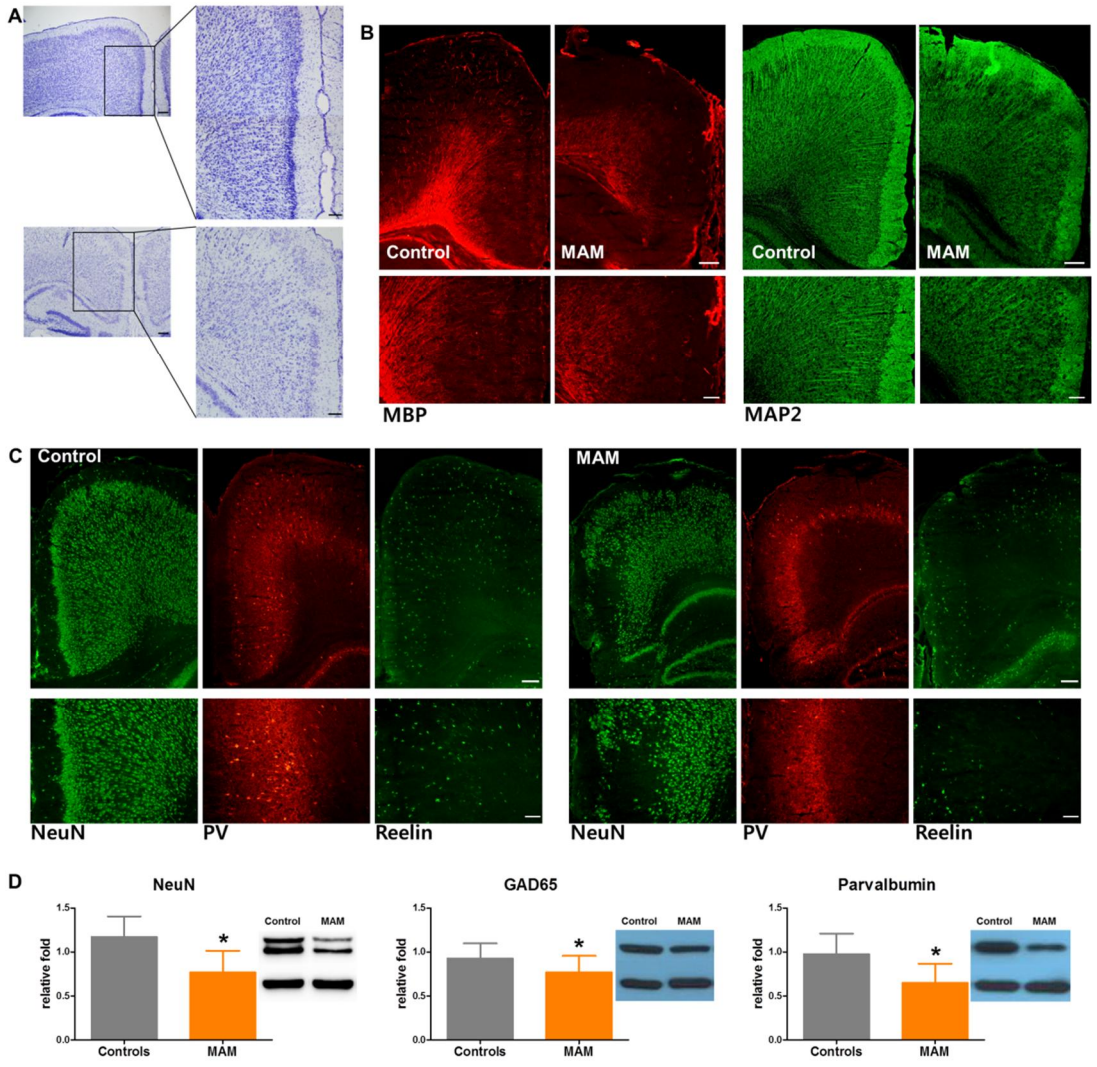

Figure 3. Morphological changes and deficiency of cortical interneurons in infant rat model of MCD. (A) Pathological alteration of cortical structure is shown by cresyl violet staining. The immunofluorescence staining with (E) MBP and (F) MAP2 also reveals microstructural disruptions of RSC in MAM treated rats at P15. (C) In infant rat with MCD, neuronal nuclei (NeuN), parvalbumin, and reelin expression in RSC

are decreased. Scale bar; lower 200μm, upper 100μm. (D) Western blot analysis shows significant reduction of NeuN ($p < 0.001$), GAD65 ($p = 0.003$), and parvalbumin ($p < 0.001$) in cortex of rat with MCD.

In RSC, infant rats with MCD ($n = 5$) show significantly decreased number of cortical neurons compared to controls ($n = 5$, $p = 0.009$, Figure 4). The pyramidal neurons of rats with MCD exhibit shorter length of apical dendrites as well as the fewer number of basal dendrites than controls (Fig. 4D, E, $n = 10$, apical dendrites; $p = 0.001$, basal dendrites; $p < 0.001$).

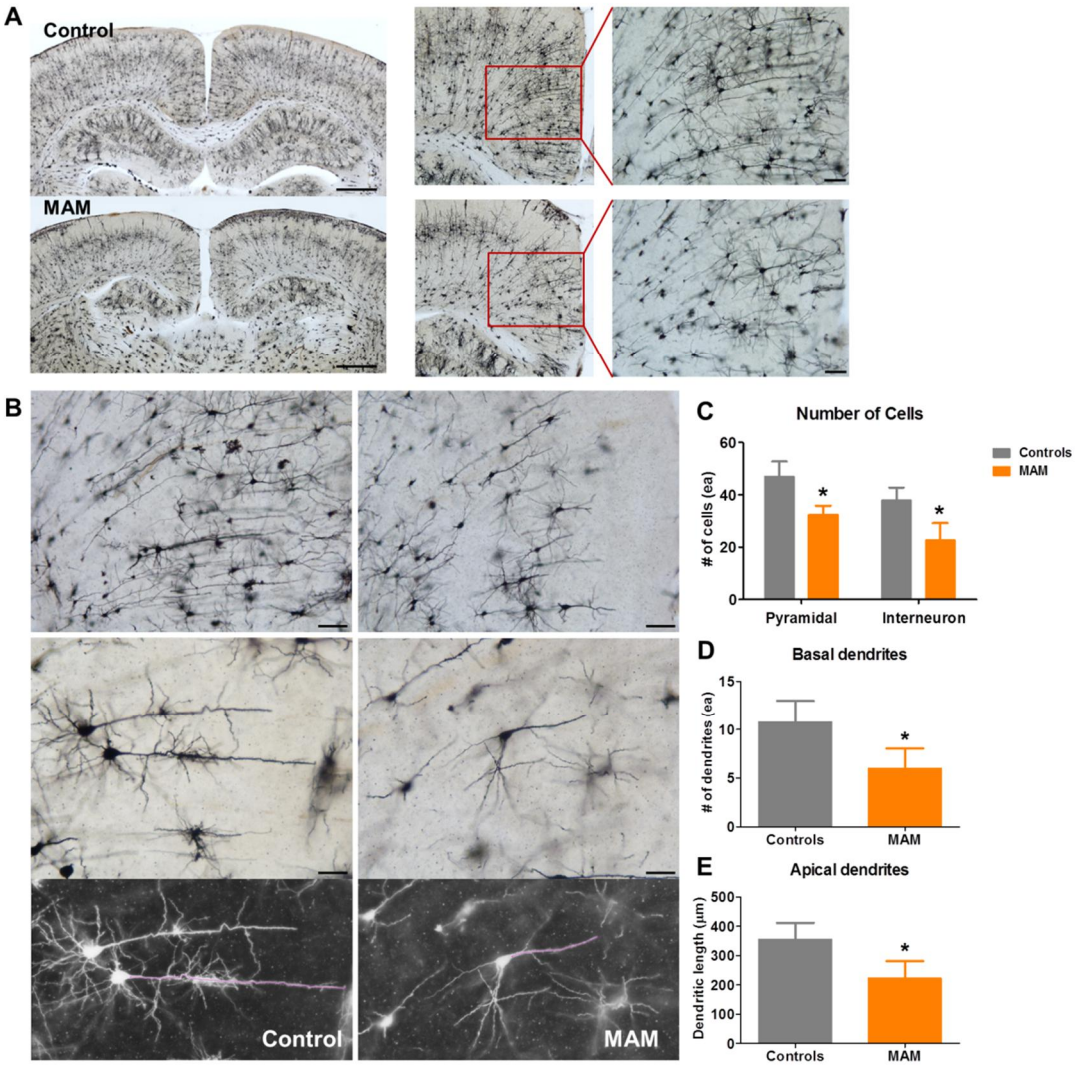

Figure 4. Dendritic arborization of RSC pyramidal cells in infant rat model of MCD. (A) Golgi staining reveals cortical neuronal deficits in infant rats with MCD. (B, C) In RSC, the numbers of pyramidal cells and interneurons are significantly reduced. (D, E) The number of basal dendrites of pyramidal cell and the length of apical dendrites are significantly reduced. Scale bar; (A) left 1㎜, right 100㎛, (B) upper 100㎛, lower

50㎛.

In vivo microstructural & neurometabolic changes of rats with MCD during infancy

In infant rats with MCD, microstructural and neurometabolic changes corresponding to pathologic data are observed. Using in vivo MR imaging data, it is confirmed that the dorsal to ventral whole brain and retrosplenial cortex (RSC) length is significantly shorter (Fig. 5A, B, C, $n = 23$, $p < 0.001$) than those of controls ($n = 24$), and FA values are significantly decreased (Fig. 5D, $n = 15$, controls; $n = 16$). MRS analysis focusing on RSC shows significant reduction of neurometabolites including glutamate ($p < 0.002$), glutamate-plus-glutamine ($p < 0.017$), NAA ($p < 0.002$), NAA-plus-NAAG ($p < 0.004$), MM09 ($p < 0.024$) and MM2-plus-Lip20 ($p < 0.027$) of infant rats with MCD ($n = 10$) compared to controls ($n = 10$, Fig. 5F). When measured in RSC, there is significantly lower GluCEST (%) of infant MAM-exposed rats ($n = 8$) than that of the controls ($n = 8$, $p < 0.001$, Fig 5G).

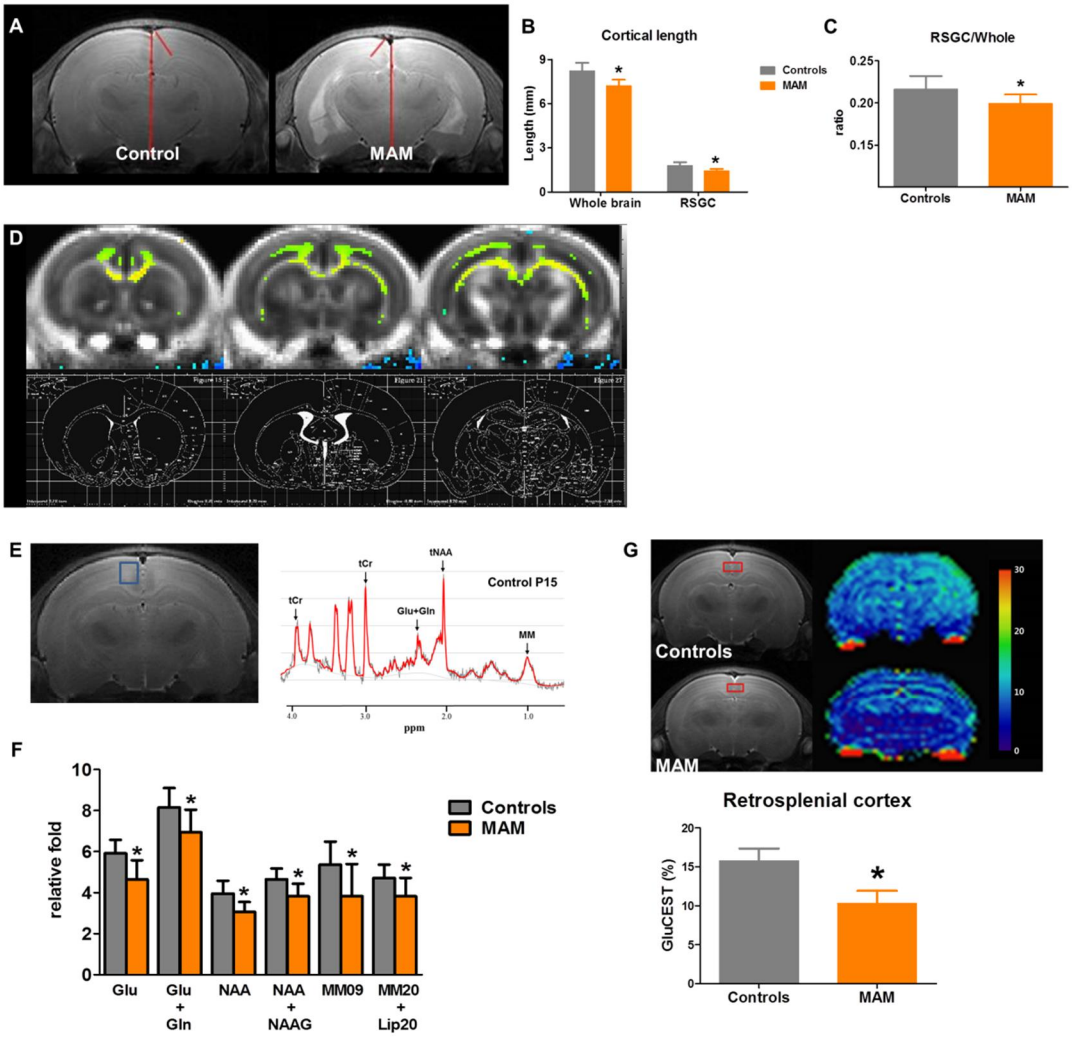

Figure 5. In vivo microstructural & neurometabolic changes of rats with MCD during infancy. (A) In representative T2-weighted magnetic resonance images, length of whole brain and retrosplenial cortex (RSC) are measured (red lines) at 3mm posterior to bregma. (B) In infant rat with MCD, length of whole brain and RSC and (C) the ratio of RSC to cortex are significantly decreased (MAM; *n* = 23, Controls; *n*

= 24, $p < 0.001$). (D) Diffusion tensor imaging reveals significant reduction of FA values in RSC of infant rat with MCD. (E) At P15, regions of interest (ROI) for magnetic resonance spectroscopy (MRS) data acquisition is depicted in the coronal, planes in the RSC (left) and an example of MR spectra is shown (right). (F) In infant rat with MCD, Glu, Glu+Gln, NAA, NAA+NAAG, MMs and Lips are significantly decreased ($p < 0.05$) compared to controls. (G) GluCEST level (%) measured from RSC (top) is significantly reduced in rat with MCD compared to controls (bottom, $p <0.001$).

Alteration of PTEN/PI3K/AKT pathway in infant rats with MCD

Cortical protein expression levels of PTEN, Akt, and downstream molecules GSK3beta, and FoxO3a are significantly decreased in infant rat with MCD ($n = 20$) compared to controls ($n = 24$, PTEN; $p = 0.022$, Akt; $p < 0.001$, GSK3β; $p = 0.036$, FoxO3a; $p = 0.005$). On the contrary to this, there are significantly increased levels of p-PTEN/PTEN and p-Akt/Akt ($p < 0.001$).

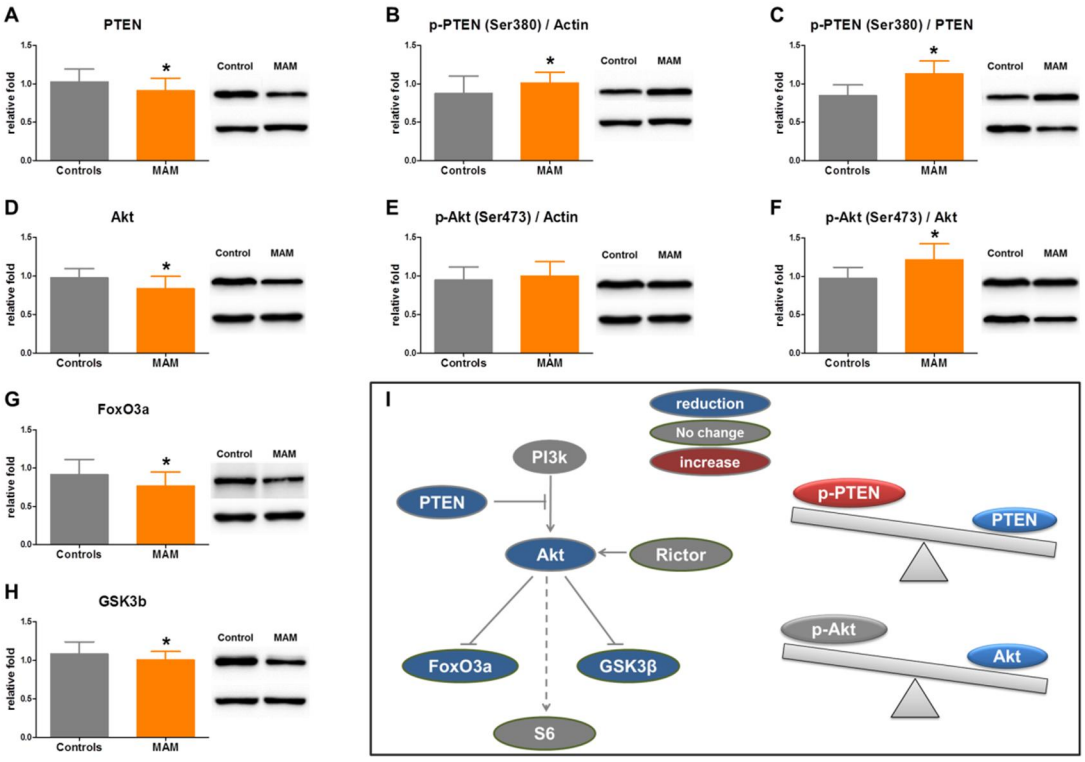

Figure 6. PTEN/PI3K/AKT pathway-related cortical protein expression in infant rats with MCD. (A, D, G, H) Cortical protein expressions of PTEN, Akt, FoxO3a, and GSK3β are significantly decreased in rat cortices of MCD compared to controls (PTEN; p = 0.022, Akt; p < 0.001, GSK3β; p = 0.036, FoxO3a; p = 0.005). (B, E) There is significant increase of p-PTEN expression (p = 0.021) and no change of p-Akt expression (p = 0.303). (C, F) p-PTEN/PTEN and p-Akt/Akt ratio is significantly elevated in rat cortices with MCD (p < 0.001). (I) Images depicting protein alterations of PTEN/PI3K/AKT pathway in cortices of infant rats with MCD.

Evaluation of the mTOR pathway in this infant rat model of MCD

In cortex of infant rats with MCD, there is no change in mTOR-related protein expression such as S6, Rictor and PI3k (Fig. 7A, B, C, D). In addition, rapamycin pretreatment with 10mg/kg for 6 days or 3mg/kg for 10 days has little effect on the number of spasms and latency to onset of spasms but significantly reduce the body weight of those treated with rapamycin (Fig. 7E, F, G).

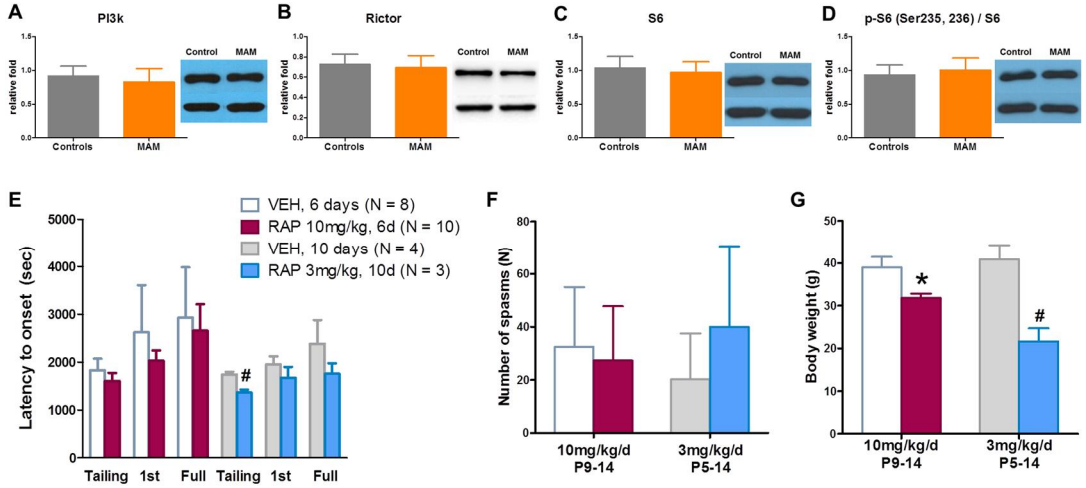

Figure 7. Evaluation of the mTOR pathway in infant rat model of MCD. (A-D) There is no significant change of PI3k, Rictor, S6 and p-S6/S6, mTOR-related cortical protein expressions in cortex of infant rat with MCD at P15. (E, F) Rapamycin

treatment with 10mg/kg for 6 days or 3mg/kg for 10 days does not affect the spasms susceptibility but significantly reduces the body weight of the rats with rapamycin (G).

Discussion

Malformation of cortical development (MCD), disruption in the developmental process of the brain, which is closely related to intractable epilepsy and developmental delay[12, 27, 28]. Many studies have shown that MCD rats using MAM have a structural abnormality similar to those observed in MCD patients, but the majority are limited to adult rats[29-31]. As epilepsy associated with MCD often occurs during infancy and is frequently refractory to current treatments[32, 33], developmental changes of MCD during infancy should be further explored.

In this study, the RSC is selected for pathological investigation to show the neocortical changes of neuronal migration, which are more likely to be associated with childhood epilepsy[9, 32]. RSC, relatively less investigated than the hippocampus, is known to be associated with default mode network and cognitive functions such as navigation, learning and memory[34]. Previous studies of the prenatal MAM-exposed MCD also reported the altered firing properties of their discrete neuronal subpopulations[6, 35].

Another study of prenatally MAM-exposed MCD rats has shown that increased spasms susceptibility and in vivo structural abnormalities, such as cortical thinning and the enlargement of ventricles, during infancy[6]. Our study also explored the pathological features of MCD at postnatal day 15. One of the histopathologic features of MCD is disorganization of the cerebral cortex architecture, such as the collapse of the cortex layer[3, 12, 27, 36] and this study identified the microcephalic feature (Fig. 5A), alteration of cortical structures (Fig. 3A), hypomyelination, and abnormalities of microtubule formation[9]. Golgi staining of RSC also showed reduced number of cortical neurons, dendritic arborization of pyramidal cells in infant rats with MCD. This result is compatible with previous study of the MAM-induced brain pathology at P12 and adulthood that showed prenatally injection of MAM leads to microcecephaly, reduced cortical thickness, and alteration of cortical pyramidal cells in morphology and their dendritic projections[36].

In addition, significant reduction of PV-positive cells in RSC was identified (Fig. 3C, D) reflecting deficiency of cortical inhibitory neurons. Although inhibitory

interneurons account for a relatively small portions of cortical cells, their dysfunction is known to cause a variety of neurological diseases including epilepsy, since they play an important role in the cortical network[7, 8]. Migration of the inhibitory interneurons into the proper layer of the cerebral cortex is one of the essential processes of cortical development to maintain the normal neural circuit activities[7, 8]. Previous studies have reported that the MAM-induced MCD model has a distorted functional connection of hippocampal-neocortical neurons[35] and alteration of interneuron migration due to aberrant $GABA_A$ activity in neocortex[37]. In this study, prenatally MAM-exposed rats also showed decreased GAD65 expression in RSC, which may be consistent with altered GABAergic activity in neocortex[38-41]. Furthermore, there was significant reduction of reelin which regulates the neuronal migration processes by controlling cell-cell interactions[38, 42-44]. These overall failures of cortical migration, dendritic arborization of pyramidal cells, and insufficient inhibitory interneurons may result in the seizure susceptibility during infancy of this model.

This study also tested whether the MCD can be diagnosed through in vivo imaging technique in clinic. There was quantified reduction of the length of the RSC as well as the dorsal to ventral whole brain length in this model using MR imaging (Fig. 5A, B, C), which can be used as the reproducible marker of MAM-induced MCD in this model[6] and also can be a diagnostic biomarker in clinic. In vivo MRI/MRS techniques also comparable findings with the pathological changes of MCD cortex. DTI also allows non-invasive identification of microstructural levels of the cerebral cortex[45, 46]. The measure of anisotropy reflects changes in myelination, dendritic architecture of cortical neuron, and fiber connection[45] and a decrease in FA values in the cortex were also observed in the patients with focal cortical dysplasia[47, 48] as in this study. Therefore, FA reduction in RSC of this MCD model (Fig. 5D) can be used as in vivo biomarker of malformed brain with abnormal myelination and dendritic arborization. Neurometabolic analysis using ^{1}H-MRS also showed reduced NAA (Fig. 5F), consistent with pathological reduction in cortical neurons identified in this study (Fig. 3C, D, Fig. 4) and previous human studies[49-51].

Both ^{1}H-MRS and GluCEST imaging revealed significantly decreased Glu and Glu+Gln in RSC (Fig. 5F, G). With its crucial function in cognition[52], glutamate, as a major excitatory neurotransmitter in central nervous system, is closely associated with epilepsy[53] and can be a useful marker of epileptic foci[54]. Glutamate also has key roles in radial migration of pyramidal neurons and tangential migration[55] and this neuro-metabolic profiles found in this study indirectly shows the abnormal cortical migration of this MAM-induced MCD rats at P15. Overall in vivo imaging data of this study could reflect the pathologic changes of MCD and these unconventional in vivo imaging can improve the diagnosis of focal cortical abnormality in patient with MCD, for example, the localization of the dysplastic cortex in patient with refractory epilepsy for epilepsy surgery.

As previously shown[6], the prenatal MAM exposed rats showed increased spasms susceptibility to NMDA during infancy. To find epileptogenic mechanisms of the epilepsy associated with MCD, the molecular changes of the cortex of MCD were investigated. The mTOR pathway is the first described genetic causes of focal

cortical dysplasia associated with epilepsy[56] and mTOR inhibitor, rapamycin has been tested as the new therapeutic option of epilepsy caused by focal cortical dysplasia[20, 57]. However, there was no significant difference of the mTOR pathway-related protein expression in MCD cortex during infancy and rapamycin pretreatment failed to alleviate the NMDA induced spasms in this study. This conflicting result between this study and previous studies of mTORopathy [10, 20, 56-59] suggested a different pathomechanism of this type of MCD other than mTORopathy. The dysplastic cortex of mTORopathy often shows pathologic findings with balloon cells or cytomegalic dysmorphic neuron forming cortical tubers or focal cortical dysplasia type II[10]. In this model, there was no cytomegalic cells but abnormal cortical migration only.

Instead, the upstream of mTOR, PTEN/PI3K/AKT pathway protein expression was significantly altered in cortex of the rats with prenatal MAM-exposed MCD (Fig. 6). PTEN/PI3K/AKT pathway is alleged to involve in the neuronal migration and focal cortical dysplasia[18, 22, 60]. Thus, altered PTEN/PI3K/AKT pathway may lead to

the cortical migration abnormality and increased seizure susceptibility and vice versa. In order to clarify the causal relationship between altered PTEN/PI3K/AKT pathway and seizure susceptibility, further study with PTEN/PI3K/AKT pathway modulation should be needed.

This study showed deficits of cortical interneurons and dendritic arborization failures in cortex of rats with prenatal MAM exposure during infancy and corresponding in vivo MR characteristics. In vivo MR techniques used in this study should be further validated as a diagnostic biomarker of MCD. In addition, MAM-induced dysplastic cortex showed translational alteration of PTEN/PI3K/AKT pathway, which should be further validated as a possible therapeutic target of epilepsy associated with MCD.

References

1. Kandel ER. Principles of neural science. (5th ed). New York: McGraw-Hill; (2013).
2. Guerrini R, Dobyns WB. Malformations of cortical development: clinical features and genetic causes. Lancet Neurol 2014;13(7):710-26.
3. Pang T, Atefy R, Sheen V. Malformations of cortical development. Neurologist 2008;14(3):181-91.
4. Kwan KY, Sestan N, Anton ES. Transcriptional co-regulation of neuronal migration and laminar identity in the neocortex. Development 2012;139(9):1535-46.
5. Colciaghi F, Finardi A, Frasca A, Balosso S, Nobili P, Carriero G, et al. Status epilepticus-induced pathologic plasticity in a rat model of focal cortical dysplasia. Brain 2011;134:2828-43.
6. Kim EH, Yum MS, Lee M, Kim EJ, Shim WH, Ko TS. A New Rat Model of Epileptic Spasms Based on Methylazoxymethanol-Induced Malformations of Cortical Development. Front Neurol 2017;8:271.
7. Wamsley B, Fishell G. Genetic and activity-dependent mechanisms underlying interneuron diversity. Nat Rev Neurosci 2017;18(5):299-309.
8. Kelsom C, Lu W. Development and specification of GABAergic cortical interneurons. Cell Biosci 2013;3(1):19.
9. Barkovich AJ, Dobyns WB, Guerrini R. Malformations of cortical development and epilepsy. Cold Spring Harb Perspect Med 2015;5(5):a022392.
10. Iffland PH, 2nd, Crino PB. Focal Cortical Dysplasia: Gene Mutations, Cell Signaling, and Therapeutic Implications. Annu Rev Pathol 2017;12:547-71.
11. Luhmann HJ. Models of cortical malformation--Chemical and physical. J Neurosci Methods 2016;260:62-72.
12. Kuzniecky R. Epilepsy and malformations of cortical development: new developments. Curr Opin Neurol 2015;28(2):151-7.
13. Chevassus-au-Louis N, Baraban SC, Gaiarsa JL, Ben-Ari Y. Cortical malformations and epilepsy: new insights from animal models. Epilepsia 1999;40(7):811-21.

14. Germano IM, Sperber EF. Increased seizure susceptibility in adult rats with neuronal migration disorders. Brain Res 1997;777(1-2):219-22.
15. Colacitti C, Sancini G, DeBiasi S, Franceschetti S, Caputi A, Frassoni C, et al. Prenatal methylazoxymethanol treatment in rats produces brain abnormalities with morphological similarities to human developmental brain dysgeneses. J Neuropathol Exp Neurol 1999;58(1):92-106.
16. Crino PB. The enlarging spectrum of focal cortical dysplasias. Brain 2015;138(Pt 6):1446-8.
17. Roy A, Skibo J, Kalume F, Ni J, Rankin S, Lu Y, et al. Mouse models of human PIK3CA-related brain overgrowth have acutely treatable epilepsy. Elife 2015;4.
18. Jansen LA, Mirzaa GM, Ishak GE, O'Roak BJ, Hiatt JB, Roden WH, et al. PI3K/AKT pathway mutations cause a spectrum of brain malformations from megalencephaly to focal cortical dysplasia. Brain 2015;138(Pt 6):1613-28.
19. Wang L, Zhou K, Fu Z, Yu D, Huang H, Zang X, et al. Brain Development and Akt Signaling: the Crossroads of Signaling Pathway and Neurodevelopmental Diseases. J Mol Neurosci 2017;61(3):379-84.
20. Nguyen LH, Brewster AL, Clark ME, Regnier-Golanov A, Sunnen CN, Patil VV, et al. mTOR inhibition suppresses established epilepsy in a mouse model of cortical dysplasia. Epilepsia 2015;56(4):636-46.
21. Lasarge CL, Danzer SC. Mechanisms regulating neuronal excitability and seizure development following mTOR pathway hyperactivation. Front Mol Neurosci 2014;7:18.
22. Itoh Y. A balancing Akt: How to fine-tune neuronal migration speed. Neurogenesis (Austin) 2016;3(1):e1256854.
23. Chang N, El-Hayek YH, Gomez E, Wan Q. Phosphatase PTEN in neuronal injury and brain disorders. Trends Neurosci 2007;30(11):581-6.
24. Garcia-Junco-Clemente P, Golshani P. PTEN: A master regulator of neuronal structure, function, and plasticity. Commun Integr Biol 2014;7(1):e28358.
25. Fraser MM, Bayazitov IT, Zakharenko SS, Baker SJ. Phosphatase and tensin homolog, deleted on chromosome 10 deficiency in brain causes defects in

synaptic structure, transmission and plasticity, and myelination abnormalities. Neuroscience 2008;151(2):476-88.

26. Terpstra M, Rao R, Tkac I. Region-specific changes in ascorbate concentration during rat brain development quantified by in vivo (1)H NMR spectroscopy. NMR Biomed 2010;23(9):1038-43.

27. Barkovich AJ, Guerrini R, Kuzniecky RI, Jackson GD, Dobyns WB. A developmental and genetic classification for malformations of cortical development: update 2012. Brain 2012;135(Pt 5):1348-69.

28. Becker AJ, Beck H. New developments in understanding focal cortical malformations. Curr Opin Neurol 2018;31(2):151-5.

29. Lodge DJ, Grace AA. Gestational methylazoxymethanol acetate administration: a developmental disruption model of schizophrenia. Behav Brain Res 2009;204(2):306-12.

30. Moore H, Jentsch JD, Ghajarnia M, Geyer MA, Grace AA. A neurobehavioral systems analysis of adult rats exposed to methylazoxymethanol acetate on E17: implications for the neuropathology of schizophrenia. Biol Psychiatry 2006;60(3):253-64.

31. Chin CL, Curzon P, Schwartz AJ, O'Connor EM, Rueter LE, Fox GB, et al. Structural abnormalities revealed by magnetic resonance imaging in rats prenatally exposed to methylazoxymethanol acetate parallel cerebral pathology in schizophrenia. Synapse 2011;65(5):393-403.

32. Kang JW, Rhie SK, Yu R, Eom S, Hong W, Kim SH, et al. Seizure outcome of infantile spasms with focal cortical dysplasia. Brain Dev 2013;35(8):816-20.

33. Tassi L, Colombo N, Garbelli R, Francione S, Lo Russo G, Mai R, et al. Focal cortical dysplasia: neuropathological subtypes, EEG, neuroimaging and surgical outcome. Brain 2002;125(Pt 8):1719-32.

34. Sugar J, Witter MP, van Strien NM, Cappaert NL. The retrosplenial cortex: intrinsic connectivity and connections with the (para)hippocampal region in the rat. An interactive connectome. Front Neuroinform 2011;5:7.

35. Chevassus-Au-Louis N, Congar P, Represa A, Ben-Ari Y, Gaiarsa JL. Neuronal

migration disorders: Heterotopic neocortical neurons in CA1 provide a bridge between the hippocampus and the neocortex. P Natl Acad Sci USA 1998;95(17):10263-8.

36. Garbossa D, Vercelli AS. Experimentally-induced microencephaly: effects on cortical neurons. Brain Res Bull 2003;60(4):329-38.

37. Abbah J, Juliano SL. Altered migratory behavior of interneurons in a model of cortical dysplasia: the influence of elevated GABAA activity. Cereb Cortex 2014;24(9):2297-308.

38. Wieronska JM, Branski P, Siwek A, Dybala M, Nowak G, Pilc A. GABAergic dysfunction in mGlu7 receptor-deficient mice as reflected by decreased levels of glutamic acid decarboxylase 65 and 67kDa and increased reelin proteins in the hippocampus. Brain Res 2010;1334:12-24.

39. Stork O, Ji FY, Kaneko K, Stork S, Yoshinobu Y, Moriya T, et al. Postnatal development of a GABA deficit and disturbance of neural functions in mice lacking GAD65. Brain Research 2000;865(1):45-58.

40. Ji FY, Kanbara N, Obata K. GABA and histogenesis in fetal and neonatal mouse brain lacking both the isoforms of glutamic acid decarboxylase. Neurosci Res 1999;33(3):187-94.

41. Silva AV, Sanabria ERG, Cavalheiro EA, Spreafico R. Alterations of the neocortical GABAergic system in the pilocarpine model of temporal lobe epilepsy: Neuronal damage and immunocytochemical changes in chronic epileptic rats. Brain Res Bull 2002;58(4):417-21.

42. Niu S, Yabut O, D'Arcangelo G. The Reelin signaling pathway promotes dendritic spine development in hippocampal neurons. J Neurosci 2008;28(41):10339-48.

43. Wasser CR, Herz J. Reelin: Neurodevelopmental Architect and Homeostatic Regulator of Excitatory Synapses. J Biol Chem 2017;292(4):1330-8.

44. Lee GH, D'Arcangelo G. New Insights into Reelin-Mediated Signaling Pathways. Frontiers in Cellular Neuroscience 2016;10.

45. Huppi PS, Dubois J. Diffusion tensor imaging of brain development. Semin Fetal Neonatal Med 2006;11(6):489-97.

46. Kharatishvili I, Immonen R, Grohn O, Pitkanen A. Quantitative diffusion MRI of hippocampus as a surrogate marker for post-traumatic epileptogenesis. Brain 2007;130(Pt 12):3155-68.

47. Donkels C, Pfeifer D, Janz P, Huber S, Nakagawa J, Prinz M, et al. Whole Transcriptome Screening Reveals Myelination Deficits in Dysplastic Human Temporal Neocortex. Cereb Cortex 2017;27(2):1558-72.

48. Lee SK, Kim DI, Mori S, Kim J, Kim HD, Heo K, et al. Diffusion tensor MRI visualizes decreased subcortical fiber connectivity in focal cortical dysplasia. Neuroimage 2004;22(4):1826-9.

49. Woermann FG, McLean MA, Bartlett PA, Barker GJ, Duncan JS. Quantitative short echo time proton magnetic resonance spectroscopic imaging study of malformations of cortical development causing epilepsy. Brain 2001;124(Pt 2):427-36.

50. Mueller SG, Laxer KD, Barakos JA, Cashdollar N, Flenniken DL, Vermathen P, et al. Metabolic characteristics of cortical malformations causing epilepsy. J Neurol 2005;252(9):1082-92.

51. Blu¨ml S, Panigrahy A. MR spectroscopy of pediatric brain disorders. New York: Springer; (2013).

52. Pepin J, Francelle L, Carrillo-de Sauvage MA, de Longprez L, Gipchtein P, Cambon K, et al. In vivo imaging of brain glutamate defects in a knock-in mouse model of Huntington's disease. Neuroimage 2016;139:53-64.

53. Eid T, Gruenbaum SE, Dhaher R, Lee TW, Zhou Y, Danbolt NC. The Glutamate-Glutamine Cycle in Epilepsy. Adv Neurobiol 2016;13:351-400.

54. Davis KA, Nanga RP, Das S, Chen SH, Hadar PN, Pollard JR, et al. Glutamate imaging (GluCEST) lateralizes epileptic foci in nonlesional temporal lobe epilepsy. Sci Transl Med 2015;7(309):309ra161.

55. Luhmann HJ, Fukuda A, Kilb W. Control of cortical neuronal migration by glutamate and GABA. Front Cell Neurosci 2015;9:4.

56. Crino PB. mTOR: A pathogenic signaling pathway in developmental brain malformations. Trends Mol Med 2011;17(12):734-42.

57. Curatolo P, Moavero R. mTOR inhibitors as a new therapeutic option for epilepsy. Expert Rev Neurother 2013;13(6):627-38.
58. Rensing N, Han L, Wong M. Intermittent dosing of rapamycin maintains antiepileptogenic effects in a mouse model of tuberous sclerosis complex. Epilepsia 2015;56(7):1088-97.
59. Ruppe V, Dilsiz P, Reiss CS, Carlson C, Devinsky O, Zagzag D, et al. Developmental brain abnormalities in tuberous sclerosis complex: a comparative tissue analysis of cortical tubers and perituberal cortex. Epilepsia 2014;55(4):539-50.
60. Ljungberg MC, Sunnen CN, Lugo JN, Anderson AE, D'Arcangelo G. Rapamycin suppresses seizures and neuronal hypertrophy in a mouse model of cortical dysplasia. Dis Model Mech 2009;2(7-8):389-98.

Appendix

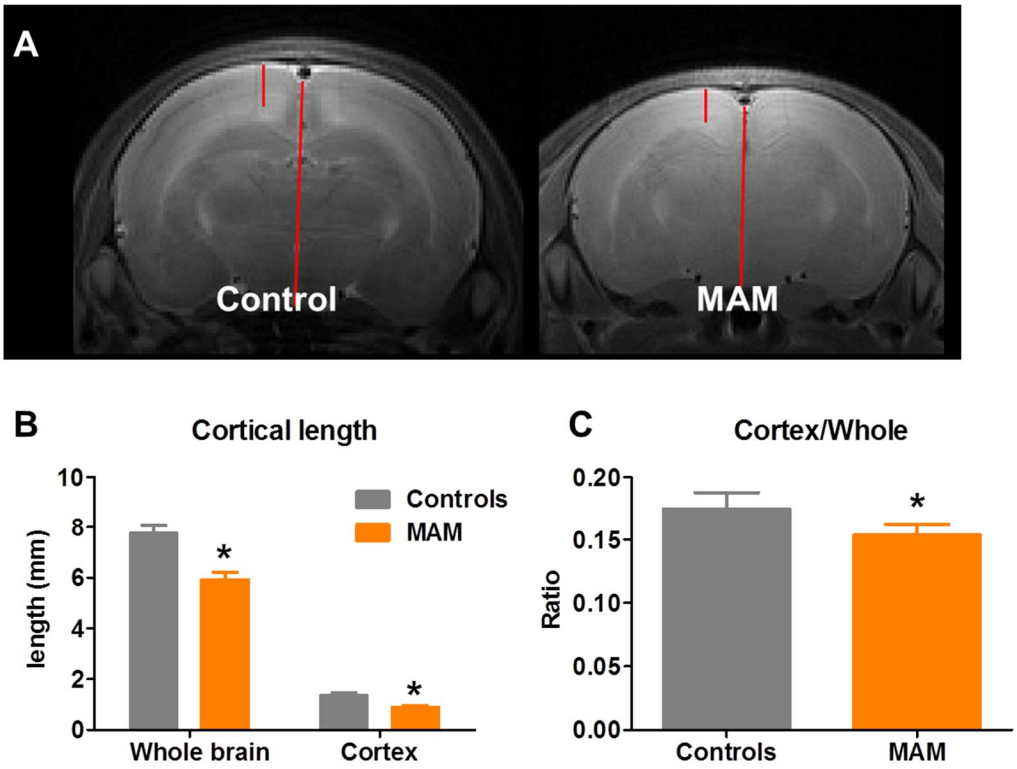

The length of whole brain and cortex on MR imaging was measured in the MAM-exposed rats (n = 26) used for rapamycin pretreatment at postnatal day 8. The rats with rapamycin or vehicle pretreatment showed significant decreased brain size compared to normal controls (n = 19, the Mann-Whitney's *U* test, $p < 0.001$).

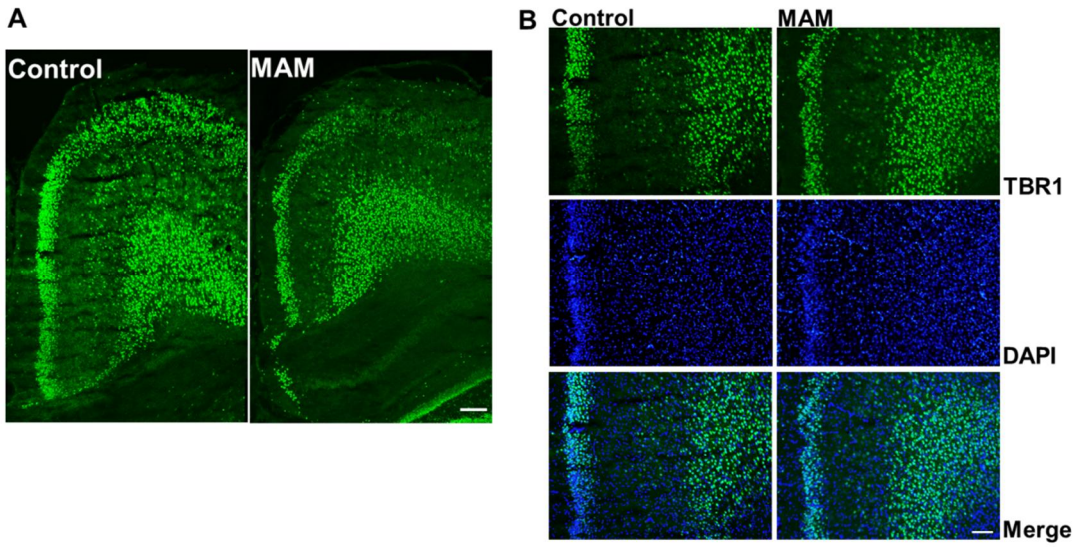

The immunofluorescence staining with TBR1 was performed in infant rat with MAM exposure and compared to normal controls at P15. Scale bar (A) 200㎛, (B) 100㎛.

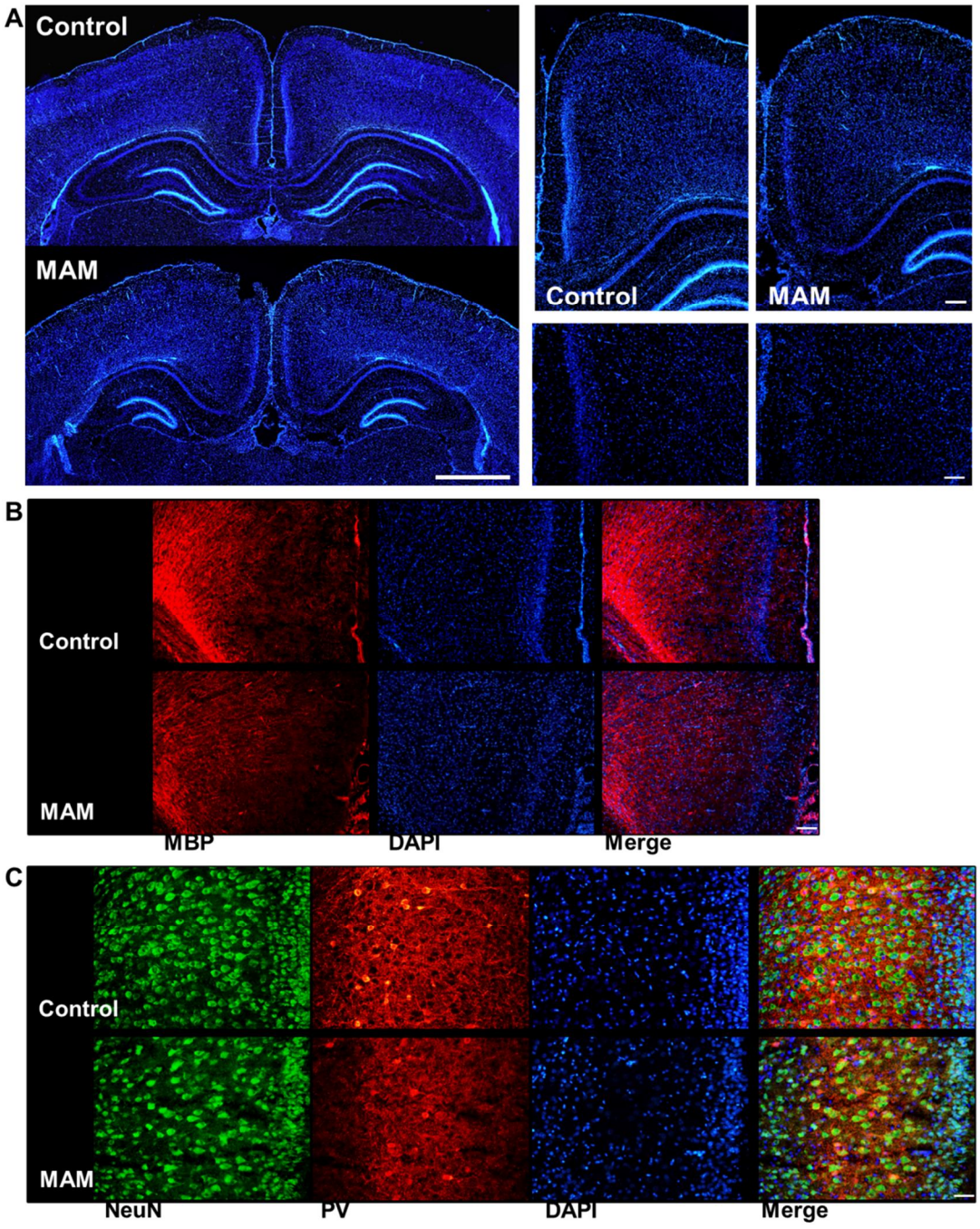

Figure 3. Additional immunofluorescence staining data in infant rat model of MCD and controls

(A) DAPI staining shows absence of corpus callosum and decreased cortical length

in infant rat model of MCD compared to controls. Dorsal neocortical layer II-III of rats with MCD is relatively shorter than the normal controls. Scale bar; left 1㎜, right upper 200㎛, lower 100㎛.

(B) MBP staining was merged with DAPI staining in Figure 2B. Scale bar 100㎛.

(C) Significant reduction of NeuN (+) and PV (+) cells in retropslenial cortex at P15 was shown in Figure 3C. Scale bar 50㎛.

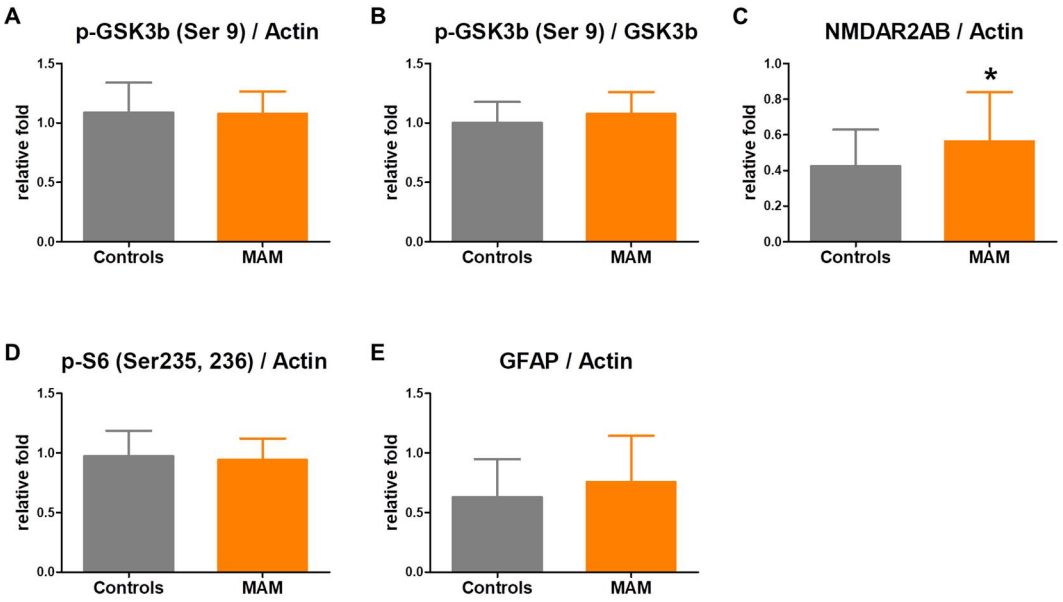

Additional western blot data in cortex of infant rats with MCD. There was no significant difference in cortical protein expression of p-GSK3b (Ser 9), NMDAR2B,

p-S6 (Ser235, 236), GFAP between rats with MCD and controls at P15.

(A) $p = 0.503$, (B) $p = 0.129$, (C) $p = 0.035$, (D) $p = 0.590$, (E) $p = 0.183$.

Korean Abstract (국문요약)

배경: 대뇌피질 발달 기형 (malformation of cortical development, MCD)은 뇌전증 발작 (epileptic seizure)을 포함하는 난치성 뇌전증의 중요한 원인 중 하나이다. Methylazoxymethanol (MAM)을 산전투여한 쥐는 대뇌피질 발달 기형의 동물모델로서 사용되고 영아기에 N-methyl-D-aspartate (NMDA)에 대한 발작 감수성 (seizure susceptibility)이 증가함을 확인하였다.

목표: 본 연구의 목적은 대뇌피질 발달 기형 동물모델의 영아기의 뇌에서 병리학적 변화를 확인하고 그와 함께 생체 내 신경대사물질의 변화를 확인하고자 하였다. 대뇌피질 발달 기형 동물 모델의 영아기에 증가된 발작 감수성 메커니즘을 이해하기 위해 분자생물학적 변화를 확인하였다.

방법: 임신 15일된 임신 쥐에게 MAM (15mg/kg IP)을 복강 내로 투여하여 MCD를 유도하고 대조군을 위해 임신 15일 된 임신 쥐에게 생리식염수를 투여하였다. 대뇌피질 이상이 확인된 쥐들과 정상 대조군에서 생후 15일에 7T 소동물 영상 시스템 (small-animal imaging system)을 이용하여 ^{1}H-MR spectroscopy (1H-MRS), diffusion tensor imaging (DTI), chemical exchange saturation transfer of glutamate (GluCEST) 영상을 획득하고 이 결과를 대조 분석하였다. 일부 동물은 동일한 시기에 희생하여 피질에서 the PI3K/AKT/mTOR pathway관련 단백질의 발현을 확인하였다. 산전에 MAM 노출된 쥐에서 라파마이신 (rapamycin)을 두 가지 투약 요법 (3mg/kg; P5 to P14, 10mg/kg; P9 to P14)으로 사전치료하고 생후 15일에 NMDA를 투약하여 90분간 연축 횟수 및 연축 발생시간을 조사하였다.

결과: 생후 15일에 대뇌피질 발달 기형 쥐의 retrosplenial cortices (RSC)에서 면역형광염색기법을 통하여 neuronal nuclei (NeuN), parvalbumin, reelin를 가진 세포가 감소한 것을 확인하였다. ^{1}H-MRS와 GluCEST를 시행한 결과, 대뇌피질 발달 기형의 영아기 쥐의 RSC에서 glutamate (Glu, p = 0.002), glutamate-plus-

glutamine (Glu+Gln, p = 0.017), N-acetylaspartate (NAA, p = 0.002), N-acetylaspartate-plus-N-acetylaspartylglutamate (NAA+NAAG, p = 0.004), macromolecules (MM) and lipids (Lips, $p < 0.05$) 레벨이 감소하고 GluCEST (%, $p < 0.001$) 레벨도 감소하였다. 그리고 phosphatase and tensin homolog (PTEN), Akt, FoxO3a, 그리고 GSK3β의 단백질 발현이 대뇌피질 발달 기형을 가진 영아기 쥐의 피질에서 대조군에 비해 감소한 것을 확인하였다. 그러나, 라파마이신 사전치료는 NMDA에 의한 발작 감수성에 영향을 미치지 못하였으며, 산전에 MAM에 노출된 새끼 쥐의 피질에서 pS6/S6, S6, Rictor, PI3k의 발현은 변화가 없었음을 확인하였다.

결론: 산전에 MAM에 노출된 영아기의 쥐에서, GABAergic interneurons의 감소와 함께 비정상적인 피질 신경세포 이주와 생체 내 영상의 특징을 확인하였다. 또한 산전에 MAM의 노출은 영아기에 PTEN/PI3K/AKT pathway의 초래하며, 이는 향후 MCD와 관련된 뇌전증 치료의 타겟으로서 연구될 수 있겠다.

중심단어: methylazoxymethanol acetate (MAM), malformation of cortical development (MCD), PTEN, AKT, animal model